Partial Melting in the Iron-Sulfur System at High Pressure: A Synchrotron X-ray Diffraction Study

Andrew J. Campbell[1,*], Christopher T. Seagle[2], Dion L. Heinz[2,3], Guoyin Shen[4], and Vitali B. Prakapenka[5]

[1]Department of Geology, University of Maryland, College Park, MD 20742
[2]Department of the Geophysical Sciences, University of Chicago, Chicago, IL 60637
[3]James Franck Institute, University of Chicago, Chicago, IL 60637
[4]HPCAT, Carnegie Institution of Washington, Washington, DC 20008
[5]Consortium for Advanced Radiation Sources, University of Chicago, Chicago, IL 60637

*Corresponding author: email = ajc@umd.edu; fax = (301) 314-9661

Submitted to Physics of the Earth and Planetary Interiors, 3 Aug 2006
Revised, 2 April 2007
Accepted, 3 April 2007

Abstract

Partial melting in the Fe-S system was investigated at high pressures because of its importance to understanding the formation, composition, and thermal structure of the Earth's core. Earlier studies at very high pressure (> 25 GPa) took place before the discovery of Fe_3S, which compromised the interpretation of those results. Furthermore, they relied on textural criteria for melting that are difficult to apply at high pressure. In this study synchrotron x-ray diffraction was used to monitor coexisting metal and sulfide at high pressures and temperatures, during laser heating in a diamond anvil cell. The criterion for melting was the disappearance of one of the two coexisting phases, and reappearance upon quench. Temperatures of eutectic melting between Fe and Fe_3S were bracketed in this way up to 60 GPa, and a lower bound was established at 80 GPa. The accuracy of the melting point measured in these studies was improved through modelling of the axial temperature distribution through the thickness of the sample; this indicated a ~6% correction to the spectroradiometrically determined temperature. The Fe-Fe_3S eutectic composition remains close to 15 wt% S up to 60 GPa.

1. Introduction

The Earth's core is mostly iron-nickel alloy, with a small proportion of "light element" component, whose precise composition remains uncertain. Sulfur is a leading candidate as the primary light element in the molten outer core, for several reasons. In the only examples that we have of planetary cores, the iron meteorites, sulfur is a primary constituent. Sulfur easily compounds with iron, producing a metallic melt at very low temperatures (1261 K eutectic temperature), which could have facilitated metallic melt segregation and core formation in the early Earth. Finally, the relatively high cosmic abundance of S (Anders and Grevesse, 1989) is not reflected in the composition of the Earth's mantle and crust, suggesting that a large amount of S may have been sequestered into the core. Alternatively, the apparent deficiency of S in the Earth may be attributed to its volatility (Dreibus and Palme, 1996; McDonough, 2003); in this case the light element in the Earth's core could consist mostly of some combination of S with other elements, likely O, Si, and/or C (McDonough, 2003).

The phase equilibria of Fe-rich systems at high pressure should present an important set of constraints on the composition of the outer core (Li and Fei, 2003). The most important feature is that the phase diagram relevant to the Earth's core must exhibit melting point depression at the pressure of the inner core / outer core boundary (136 GPa), to satisfy the observation that the inner core has properties compatible with a predominantly iron alloy. The large density difference (~7%; Masters and Gubbins, 2003) observed between the solid inner core and the liquid outer core further suggests that the system probably melts in a eutectic fashion; alternatively, a solid solution – melt phase loop would need to be very wide to account for this density difference. The temperature at which melting takes place, and other details of the phase diagrams, can likewise be used in conjunction with other mineral physics constraints to interpret more precisely the seismological profiles of the core.

Because of this relevance to understanding the Earth's core, there have been several previous experimental studies on the melting behavior of the Fe-S system at high pressure (Brett and Bell, 1969; Ryzhenko and Kennedy, 1973; Usselman, 1975; Williams and Jeanloz, 1990; Boehler, 1996; Li et al., 2001; Fei et al., 1997; 2000). However, the very high pressure (> 25 GPa) data, obtained using diamond anvil cell techniques, are deserving of re-investigation for at least two reasons. The first is that there is poor agreement among them, and also between the diamond anvil cell data and the multi-anvil press data obtained at lower pressures. The second reason is that the previous laser-heated diamond anvil cell work was obtained prior to the discovery by Fei et al. (1997; 2000) of iron sulfide compounds at high pressures that are more Fe-rich than FeS, the most important being Fe_3S. The lack of knowledge of Fe_3S is likely to have led to misinterpretations of experimental data that could have compromised the results of Williams and Jeanloz (1990) and Boehler (1996).

A summary of previous work on melting in the Fe-FeS system is presented in Figure 1. There is general agreement that at low pressures (<5 GPa), the slope of the eutectic temperature with pressure is very small (Brett and Bell, 1969; Usselman, 1975) or even slightly negative (Ryzhenko and Kennedy, 1972; Fei et al., 1997). Usselman (1975) and Fei et al. (1997; 2000) each reported an upward cusp in the slope of the eutectic temperature, but at different pressures. Usselman (1975) speculated that the change in slope observed at 5 GPa was related to a subsolidus phase transformation in FeS, but subsequent work has shown no transition at those P,T conditions. Those data of Usselman's (1975) at pressures above the kink in the eutectic temperature were obtained with a different apparatus (high-compression belt) than those data below the kink (piston-cylinder and modified belt apparatus). The increase in the eutectic temperature above 14 GPa reported by Fei et al. (1997; 2000), in data obtained from a multi-anvil press, was positively associated with the appearance of new phases, including Fe_3S_2 and Fe_3S. Williams and Jeanloz (1990) and Boehler (1996) used laser heated diamond anvil cell techniques to measure melting in the Fe-FeS system to much higher pressures, 90 and 62 GPa respectively. Boehler's (1996) data are consistent with those of Usselman (1975) in the pressure region of overlap, but they are ~400 K higher than the data of Fei et al. (1997) at 14 GPa (Fig. 1). Boehler (1996) studied a 1:1 mixture of Fe:FeS, which is more S-rich than Fe_3S and therefore would not have produced the same eutectic that was studied in the multi-anvil press at P > 20 GPa (Fei et al., 2000; Li et al., 2001). The Fe-FeS melting temperatures of Williams and Jeanloz (1990) are systematically higher than all other data. Recently Andrault et al. (2007) described experiments using techniques very similar to those discussed below, but they reported no specific melting temperatures for the Fe-S system.

In the present study, partial melting in the Fe-S system was investigated using synchrotron X-ray diffraction of laser-heated diamond anvil cell samples. The use of X-ray diffraction as an in situ high-temperature, high-pressure probe provides an alternative to the textural criteria for melting that were used in previous work. It also allows pressure determination by the equation of state of a phase inside the cell, greatly reducing the uncertainties associated with the thermal contribution to the pressure in a laser-heated diamond anvil cell. Finally, x-ray diffraction gives a direct indication of the identity of the solid phase(s) present in the sample, so there is no ambiguity about which phase is coexisting with melt during the experiment.

2. Experimental

2.1. Diffraction experiments

Most of the experimental procedures were the same as those described by Seagle et al. (2006). Mixtures of Fe and FeS were prepared by grinding the starting materials under ethanol for a few hours to a grain size of ~1 μm. The bulk compositions of the samples were Fe5wt%S, Fe10wt%S, or Fe15wt%S, but fine scale heterogeneities may have slightly disturbed this mean composition on the scale of the experiments. The powders were then pressed into a wafer between two diamond anvils. The wafer was placed between two layers of NaCl, ~15 μm thick, and loaded into a diamond anvil cell with a stainless steel, Inconel, or Re gasket. The gaskets were pre-indented to 30-40 μm thickness, and 100 μm holes were formed in the center of the indentations to serve as sample chambers. The anvil culets were 250 μm for most experiments, but 400 μm culets were used in some lower pressure experiments.

After compression the sample was studied by angle dispersive (λ = 0.3344 Å) X-ray diffraction at the GSECARS 13-ID-D beamline of the Advanced Photon Source, Argonne National Laboratory. Diffraction data were collected before, during, and after double-sided laser heating at sequentially higher temperatures (Shen et al., 2001). The incident X-ray beam was focussed to 5 μm by 7 μm at full width half maximum using Kirkpatrick-Benz mirrors. Diffraction images were collected over 4° to 22° scattering angles using an image plate detector, and processed using the programs Fit2D (Hammersley et al., 1997) and PeakFit (Systat Software Inc.). As anticipated by Shen et al. (1998), the use of an area detector was of particular advantage in this study. At high temperatures texturing is sometimes promoted in laser-heated diamond anvil cell experiments, and energy dispersive diffraction, at a single fixed position, is susceptible to missing diffraction peaks under such circumstances (Shen et al., 1998). Area detectors are much better suited to recording spotty diffraction patterns, as were observed in this study, because they cover a far greater fraction of the diffraction cones.

The Nd:YLF laser beams were focussed to a ~30 μm spot on both sides of the sample. Coalignment of the X-ray beam and the laser-heating/temperature measurement system was accomplished with the aid of X-ray induced fluorescence from the NaCl pressure medium, viewed through the temperature measurement portion of the optical system (Shen et al., 2005). Temperatures were determined spectroradiometrically (Heinz and Jeanloz, 1987a), from light emitted from the central 5 μm of the laser heated spot on both sides of the sample (Shen et al., 2001). The area of the sample probed by X-ray diffraction was therefore similar to the area measured spectroradiometrically, and much smaller than the laser heated spot, minimizing errors associated with radial temperature gradients in the laser-heated cell. Calibration of the optical system used for temperature measurement was performed using a spectrally calibrated tungsten filament lamp (Shen et al., 2001).

Before collection of each X-ray diffraction pattern was initiated, the laser powers on both sides of the cell were adjusted to minimize the axial gradient in temperature as much as possible. In practice, the difference between downstream (of the X-ray beam) and upstream temperatures varied from 2 to 100 K. The reported values are the averages of upstream and downstream temperature measurements, corrected by ~6% to account for the remaining axial gradient through the sample (see Section 2.3 below).

The uncertainties in the spectroradiometric temperature measurement were estimated to be ±100 K based on the precision of the system as described by Shen et al. (2001). This is based on their tests of laser heating thermocouple junctions, and also melting pure metals by laser heating at 1 bar. The error associated with the spectroradiometric fit was negligible in comparison. An additional uncertainty exists with regard to the axial temperature gradient through the sample (Section 2.3), which depends on the sample thickness (4 to 10 μm). Our overall uncertainty on the temperature measurements is ±140 K.

Pressures were calculated from the lattice parameters of Fe, using its high-temperature, high-pressure equation of state. A description of the equation of state parameterization used for the pressure calibration was given by Seagle et al. (2006), and it is based on the shock wave data summarized by Brown et al. (2000) and the room temperature compression curve of Mao et al. (1990). Similar pressures were determined using the measured NaCl lattice parameters and assuming 300 K for the temperature of the non-absorbing pressure medium. However, because of the uncertainty regarding the actual range of temperatures (and large T gradient) experienced by the NaCl during heating, we only report pressures based on the high-P,T equation of state of Fe. It is conceivable that some solid solution of S into the Fe crystal structure might occur at high pressures and temperatures, and it is important that this possibility be considered. However, the phase diagram study of Li et al. (2001) indicated that, at least up to 25 GPa, the solid solution of S into Fe is very small (≤1.4 at%). Furthermore, Seagle et al. (2006) demonstrated that Fe_3S and hcp-Fe have very similar mean atomic volumes (within 3% from 21 to 82 GPa), indicating that any solid solution that does exist has a negligible effect on the lattice parameters, and therefore does not significantly impact the use of Fe as an internal pressure standard (≤0.6 GPa).

After compression, each sample was heated to sequentially higher temperatures for a series of diffraction patterns. Ordinarily the laser power was increased slowly over a period of a couple of minutes, and the final temperature for the diffraction measurement was held for 3-5 minutes. Following each X-ray diffraction exposure, the sample was quenched by closing the laser shutter, while the image plate was read. After readout a diffraction pattern of the quenched sample was obtained, and then the laser heating cycle began again, to a new (usually higher) temperature. The temperature interval between heating steps was typically 50-200 K. When melting was achieved (based on examination of the diffraction image), the sample was compressed to higher pressures, and a laser heating cycle began anew. Effort was made to avoid reheating a portion of a sample that had previously been laser-heated at a lower pressure.

2.2. Criterion for melting

The criterion for melting in these experiments was the disappearance of either sulfide or metal, with the other phase remaining visible in the diffraction pattern. The use of an area detector in this study was a great advantage over earlier work using in situ X-ray diffraction as a melting criterion (Shen et al., 1998), because detection of the full 2θ scattering cones helped avoid problems associated with coarsening of the sample grain size and consequent spottiness of the diffraction pattern. Diffuse scattering from the melt is much weaker than diffraction from the remaining crystalline phases in these experiments.

The duration of laser heating at each temperature step was typically 3-5 minutes. The ability of the sample to melt during this time depends on the diffusion rates in the starting materials. Diffusion rates are difficult to estimate in these materials because they have not been measured in the relevant high-pressure phases, either at 1 bar or at high pressure. However, our observations indicate that there was ample time for diffusive equilibration of the fine-grained samples (~1 μm or less before heating). In all experiments, even at the lowest heating conditions, after heating the diffraction pattern was observed to become very spotty compared to the uniform diffraction ring that is observed at room temperature before laser heating. This is an inconvenience that necessitates the use of an area detector, as described above, but it also reveals that the sample grains were able to recrystallize extensively during heating. We take this as evidence that the diffusion rates during our experiments were sufficiently high that the samples were able to achieve, locally, their equilibrium state. Later experiments have shown that the spottiness of the diffraction pattern, hence diffusive re-equilibration, is achieved even when the heating duration is only a few seconds (Seagle, unpublished work). There is no evidence that the fine-grained samples in our experiments was superheated, maintaining the solid state above the melting point for the duration of the experiment.

In all cases, it was the Fe metal that remained upon partial melting of the sample, indicating that our sample compositions were on the Fe-rich side of the eutectic. The sulfide phase that coexists with Fe before melting at high pressure is Fe_3S (Fei et al., 2000), although at lower temperatures we also observed FeS that had not yet been consumed by reaction with Fe to form the Fe_3S. After quenching from the partially molten state, Fe_3S was observed to reappear in the diffraction patterns. This is an important observation, because it indicates that the sulfur remained present in the laser heated spot during heating; its absence at high temperatures was not a consequence of some other experimental artifact, like Soret diffusion (Heinz and Jeanloz, 1987b) or migration of melt (Campbell et al., 1992). We also note that the bracketing of eutectic temperatures is insensitive to variations in the starting composition. Eutectic melting occurs at the same temperature anywhere along the compositional join, so if there are minor heterogeneities in the Fe-FeS mixtures that comprise the starting material, these will not affect our results.

2.3. Correction for axial temperature gradient

In these experiments, the samples were laser-heated from both sides. Independent adjustment of the laser power incident on either side allowed the temperatures at the two surfaces to be balanced. However, because radial heat flow is permitted by the sample geometry, it is likely that the interior temperatures in the sample are somewhat lower than the measured surface temperatures; i.e., there can be an axial temperature gradient through the sample. This can affect our phase diagram studies, because the x-ray diffraction measurements are an integration of signals throughout the thickness of the sample, within the 5 μm x 7 μm spot size of the x-ray beam.

The magnitude of the axial temperature gradient in samples like ours (double-sided heating; opaque phases) has not been previously considered in detail. Several authors have calculated temperature gradients in dielectric samples that were laser heated (Bodea and Jeanloz, 1989; Panero and Jeanloz, 2001; 2002; Kiefer and Duffy, 2005), but the opacity of the metal phases being heated in the present study caused all of the laser radiation to be absorbed at the surface of the sample, not throughout the sample as in the dielectric samples previously considered. Morishima and Yusa (1998) calculated axial gradients in a metal that was heated from one side only. They found that the result is a strong function of the laser spot size; under typical laser heating conditions, a ~15 μm diameter hotspot imposed a temperature difference of 340 K from front to back of the sample, but with a ~60 μm hotspot the axial gradient was only 30 K. It is difficult to apply Morishima and Yusa's (1998) results to the present experiments, because we can expect that the double sided heating technique will significantly reduce the axial gradients. Therefore it was necessary to model the temperature distribution within a metallic diamond anvil cell sample that is laser heated from both sides.

In this calculation we assume that both surfaces of the sample (thickness *d*) were heated by identical, Gaussian temperature profiles:

$$T - 300 = T_0 \exp[(-r^2)/(2w^2)] ,$$

where T_0+300 is the peak temperature, r is radial distance, and w is the characteristic length scale of the radial temperature gradient. Accordingly, the steady-state temperature distribution within the sample is expected to be of the radially symmetric form:

$$T - 300 = F(r,z)\, T_0 \exp\,[(-r^2)/(2w^2)]$$

where $F(r,z)$ is unknown. Substituting this into the heat equation yields

$$F_{zz} + F_{rr} + (1/r - r/w^2)\, F_r + (r^2/w^4 - 2/w^2)\, F = 0$$

where subscripts indicate partial derivatives. The following boundary conditions were applied: $F(r,0) = 1$ to satisfy the surface condition of temperature distribution; $F_z(r,d/2) = 0$ to balance heat flow from the two surfaces; $F_r(0,z) = 0$ enforces the radially symmetric solution; and $F(r,z) = F(r,d-z)$ enforces a solution symmetric about the sample midplane ($z = d/2$).

A numerical solution for typical laser heating conditions (T_{max} = 2000 K; thickness d = 7 μm; hotspot diameter $2w$ = 30 μm) is shown in Figure 2. In this solution, along the laser heating axis the minimum temperature is 1911 K (ΔT = 89 K). In general, the thermal distribution shown in Figure 2 can be scaled by a factor (T_{max}-300)/(2000-300) for peak temperatures other than 2000 K; in other words, the minimum temperature increase along the heating axis is 5% lower than that at the surface. This result is a good estimate for our typical experimental conditions. Other scenarios include increasing the sample thickness to 10 μm, which increases ΔT along the axis to 10%, or decreasing the hotspot diameter to 20 μm, which increases it to 11%. A thinner sample or a larger hotspot diameter reduces the axial gradient accordingly; for example, a 4 μm thick sample reduces the axial gradient to only 2%. As stated in Section 2.1 above, our measured temperatures were corrected downward by 6±6% to account for the presence of cooler material being probed by the x-ray beam passing through the thickness of the sample.

3. Results

The results of our experiments on the partial melting in the Fe-S system at high pressures are listed in Table 1. The reported data include the highest temperatures at which both metal and sulfide were observed to persist in the diffraction patterns, and the lowest temperatures at which sulfide was observed to be absent from the diffraction patterns. In addition to the pressure and temperature associated with each data point, the lattice parameters of Fe metal are also included in Table 1. This is done to facilitate future recalculation of the pressures, if desired, using updated high-P,T equations of state. Quenched samples were found to have pressures that were 8 to 18 GPa lower than the pressure of the samples just before quenching.

A set of diffraction patterns, representative of those upon which the data in Table 1 are based, are presented in Figure 3. At 1710 K, Fe, Fe_3S, and the NaCl pressure medium are all present as solid phases in the sample. As the temperature of the sample was raised from 1710 K to 2100 K, the Fe_3S phase disappears from the diffraction pattern but the hcp-Fe peaks remain. Then, upon quench of the sample from 2100 K, Fe_3S is clearly visible once again (Figure 3). This sequence of X-ray diffraction patterns illustrates the partial melting, and recrystallization upon quench, of Fe-Fe_3S at high pressure. At some temperature between 1710 and 2100 K, the eutectic temperature of the Fe-Fe_3S binary was exceeded, and partial melting occurred, leaving crystalline Fe and a sulfide melt to coexist in the spot probed by the X-ray beam. Only phases of Fe and iron sulfides, plus the pressure medium, were observed in our experiments. No additional phases were identified in the X-ray diffraction patterns recorded in this study.

The data bracketing the eutectic melting of Fe-Fe_3S at high pressures are plotted in Figure 4. The eutectic temperature increases over the pressure range of 30 to 60 GPa with a slope of ~12 K/GPa. A single experiment at 80 GPa, using a Fe15wt%S composition, provided only a lower bound on the eutectic temperature; X-ray diffraction patterns above 2100 K in this experiment were ambiguous because the hcp-Fe peaks diminished in intensity but did not completely disappear.

4. Discussion

Fei et al. (1997; 2000) and Li et al. (2001) performed multi-anvil experiments in the Fe-S system that provide important constraints on the melting behavior at lower pressures (< 25 GPa). The multi-anvil data show that the eutectic composition of the Fe-FeS system shifts to lower S contents with increasing pressure (Figure 5). At 1 bar the Fe-FeS eutectic is 31.6 wt% S (Massalski et al., 1990); at 7 GPa it is 20.7 wt% S (Fei et al., 1997). Beyond this pressure the Fe-FeS system becomes complicated by the appearance of several compounds of intermediate composition. By 21 GPa the eutectic composition has dropped to 15.4 wt% S, between Fe and Fe_3S (=16.1 wt% S), and peritectics on the S-rich side of the diagram involve the appearance of Fe_3S and $Fe_{3+x}S_2$ as liquidus phases (Fei et al., 2000). At 25 GPa the eutectic between Fe and Fe_3S has shifted farther toward Fe, to 14.7 wt% S (Li et al., 2001), but no information is available on the S-rich side of the Fe_3S divide.

The starting compositions of our samples are compared in Figure 5 to the eutectic compositions constrained by Fei et al. (1997, 2000) and Li et al. (2001) using multianvil press techniques to 25 GPa. The mixtures used in our experiments all fall between Fe and Fe_3S, so it is expected that the Fe-Fe_3S eutectic was measured. In all cases we found that, upon partial melting of the samples, the sulfide phases were eliminated from the diffraction patterns, indicating that Fe coexisted with sulfide melt. Our interpretation of this being a Fe-Fe_3S eutectic is supported by the fact that Fe_3S was the sulfide phase that was observed to reappear upon quenching of the laser heated samples. The persistence of a Fe-Fe_3S eutectic to high pressures is indicated in Figure 5 by the dashed arrow. This trend is only approximate, and it is likely that it is not linear as shown. Nonetheless, we find no evidence for any new phases between Fe and Fe_3S at higher pressures, where only Fe and Fe_3S are observed during the experiments. In the 20-60 GPa pressure range, it is apparent that the partial melting in these experiments reflects a eutectic along the Fe-Fe_3S join. We find little variation of the eutectic composition with increasing pressure, consistent with the levelling off seen at lower pressures (Figure 5).

The Fe-Fe_3S eutectic temperature does not increase linearly with pressure, but exhibits kinks when it crosses a phase boundary in one of the coexisting solids. This is evident in the multi-anvil press data (Fei et al., 1997; 2000; Li et al., 2001) shown in Figure 4, where the coexisting sulfide changes from FeS to $Fe_{3+x}S_2$. A similar kink in the eutectic temperature-pressure tend must exist at higher pressures, where it crosses the fcc-hcp phase boundary in iron. A comparison of the data in Figure 4 to the phase diagram of Shen et al. (1998) suggests that this should occur near 30 GPa, but it is not observed in our data because all of our bounds on melting lie in the hcp field of the Fe phase diagram.

It is conceivable that, somewhere along the pressure range of this study, Fe-Fe_3S melts not eutectically but at a peritectic, with a eutectic lying instead on the S-rich side of Fe_3S. There is no positive evidence to support this notion, but it cannot presently be ruled out because of a lack of data showing Fe_3S coexisting with a more Fe-rich melt. In this alternative interpretation, the melt in our experiments would have to have been quenched from a high enough temperature that its composition happened to be less S-rich than Fe_3S, causing Fe_3S to crystallize upon quench. We judge this to be less likely than the simpler interpretation of eutectic melting between Fe and Fe_3S, as observed indisputably by Fei et al. (2000) at 21 GPa. More data, including from the S-rich side of Fe_3S, will further elucidate many details of the phase relations in the Fe-FeS system at higher pressures.

Our data can be compared to those of Boehler (1996), who performed similar experiments on melting of Fe-FeS mixtures (1:1 by weight, or 18.2 wt% S) up to 60 GPa in a laser heated diamond anvil cell. As mentioned above, those experiments were done before the discovery of Fe_3S and other iron sulfide phases (Fei et al., 1997; 2000); consequently, Boehler (1996) could not have known that it was most important to study the Fe-rich side of the system (< 16 wt% S), to ensure that all of the experiments were relevant to the Fe-Fe_3S binary. Of course melting data at higher S contents (in the Fe_3S-FeS system) are also important for understanding the iron-sulfur system from a broader perspective, and perhaps directly applicable to some restricted planetary conditions, but they do not yield direct information on the Fe-Fe_3S eutectic temperature, which is likely to be more appropriate to discussions regarding the Earth's core. Boehler's (1996) data, according to his stated starting composition, probably do not represent partial melt systems with Fe metal present (Figure 5), but instead indicate the temperatures of a eutectic or peritectic in the Fe_3S-FeS join.

In addition to the differences in bulk composition, both the criteria for melting and the pressure calibrations differ between our study and that of Boehler (1996). Boehler (1996) determined the appearance of melt on the basis of textural changes on the surface of the sample during heating. The difficulty in observing textural changes is thought to have been partly responsible for significant discrepancies between melting curves reported by different experimental groups using the laser-heated diamond cell in the past (e.g., Williams et al., 1987; 1991; Boehler et al., 1993; Shen et al., 1993). We aimed in this study to promote an alternative criterion for melting, one that is less subjective. Furthermore, the observation of textural changes became increasingly difficult at high pressures in the Boehler (1996) experiments, limiting that data set to 60 GPa. The pressures reported in this study are determined in situ by X-ray diffraction determination of the unit cell volume of iron, under high pressure high temperature conditions. We regard this as an improvement over previous studies of melting in the laser-heated diamond anvil cell, in which the pressure was determined by the ruby fluorescence technique (Mao et al., 1978) at room temperature, and the thermal contribution to the pressure was unknown.

Despite all these complications, Boehler's (1996) results are compared to our Fe-Fe_3S eutectic melting data in Figure 4, and the two data sets show similar pressure-temperature slopes, with an offset amounting to 150-200 K or 10-12 GPa. There are at least two interpretations of this comparison between the data sets. The first is that the Fe-FeS mixture used by Boehler (1996) was actually more iron-rich than the stated 1:1 mixture, and the temperatures measured by him are in fact appropriate to the Fe-Fe_3S eutectic. In this case, the deviation between our data and his can be attributed to differences in the pressure calibration and/or the different criterion used to establish the onset of melting. The second possibility is that the pressure-temperature path of melting of a Fe18wt%S composition (probably a eutectic or peritectic between Fe_3S and FeS) is approximately parallel to that of the Fe-Fe_3S eutectic, but at temperatures higher by 150-200 K. In fact, a peritectic of the kind Fe_3S+liq = FeS+liq = liq could explain the offset between Boehler's (1996) data and ours. It is difficult at this stage to determine which of these two possibilities is correct. Additional experiments on melting in the Fe_3S-FeS system would possibly provide further clarification. The fortunate fact is that any interpretations of the formation, evolution, and composition of the Earth's core, that have been based on the melting curve of Boehler (1996) for the Fe-FeS system, will require only modest revision on account of our new melting data on the Fe-Fe_3S system.

On the other hand, those data that were in disagreement with Boehler's (1996) melting curve are inconsistent with our data as well. This includes the results of Williams and Jeanloz (1990), the details of whose temperature measurements and criterion for melting had previously led to disagreement with others in the case of pure Fe (Williams et al., 1987; 1991; Boehler et al., 1993; Shen et al., 1993). Williams and Jeanloz (1990) investigated melting in a Fe10wt%S mixture, comparable to the measurements reported here, so their data are definitely relevant to the Fe-Fe_3S eutectic, unlike those of Boehler

(1996). However, their data lie at much higher temperatures than those reported here and in Boehler (1996) – approximately 800 K higher at 60 GPa.

The eutectic temperatures determined by the multi-anvil experiments of Fei et al. (1997; 2000) and Li et al. (2001) to low pressures (< 25 GPa) are also compared to our data in Figure 4. At these low pressures, the laser-heating technique is less easily applied to this system, because the eutectic temperatures are so low that thermal emission becomes significantly reduced. The results of Fei et al. (1997; 2000) and Li et al. (2001) reveal that the eutectic temperature in the Fe-rich portion of the Fe-S system initially decreases mildly with increasing pressure. After the appearance of Fe_3S_2 on the solidus at 14 GPa (Fei et al., 1997), the eutectic temperature rises. At 21 GPa Fe_3S appears on the solidus (Fei et al., 2000), and the eutectic temperature in the Fe-Fe_3S system continues to rise at a rate that is consistent with the high pressure diamond anvil cell results reported here and in Boehler (1996).

Our lower melting temperatures agree with the multi-anvil press results (Fei et al., 2000; Li et al., 2001) more closely than the previous diamond anvil cell data (Boehler, 1996; Williams and Jeanloz, 1990) do. However, in the overlapping pressure range (< 25 GPa), the precision and number of eutectic temperatures from diamond anvil cell data are still permissive in their comparison with the multi-anvil data. More data using both techniques in this pressure range will allow stricter comparison to be made. A few data reported by Boehler (1996) below 20 GPa lie far above the multi-anvil press results of Fei et al. (1997; 2000); however, these could have been compromised by having bulk composition outside the Fe-Fe_3S range, as discussed above. The Williams and Jeanloz

(1990) data, which are not shown in Figure 4, are even more difficult to reconcile with the multi-anvil results, as they are 800 K higher than the Li et al. (2001) data at 25 GPa.

The temperature of the Earth's outer core must be above the eutectic temperature of the iron-rich multicomponent system that comprises the core. Comparison with our Fe-Fe_3S melting data with the melting curve of pure Fe (Shen et al., 1998; 2004; Boehler, 1993) indicates that the melting point depression of Fe, due to sulfur alloying in the melt, amounts to 700-900 K over the pressure range of our study (30 to 80 GPa). Boehler's (1993) melting curve for pure Fe is the lowest of several published curves; applying our melting point depression of 700-900 K to Boehler's (1993) melting point of Fe at the core-mantle boundary pressure (136 GPa) suggests a minimum temperature of the outer core of ≥ 2400 K, assuming S as the dominant light element in the outer core. This temperature bound is low enough to be non-controversial; most estimates of the thermal structure of the mantle easily accommodate a temperature greater than 2400 K at the core-mantle boundary (e.g., Jeanloz and Richter, 1979). Our melting point depression of 700-900 K is identical to that calculated by ab initio methods by Alfè et al. (2002), for a Fe-S-O melt at 330 GPa, the pressure of the inner core / outer core boundary. Most estimates of pure Fe melting at this pressure are in the range 5300-6700 K (Anderson and Duba, 1997; Alfè et al., 2002); applying a ~800 K melting point depression to this range implies a minimum inner core / outer core boundary temperature of 4500-5900 K.

Acknowledgments

We thank J. Devine for help in the experiments. Y. Fei and an anonymous reviewer are thanked for their useful reviews. This work was performed at GeoSoilEnviroCARS (Sector 13), Advanced Photon Source (APS), Argonne National Laboratory. GeoSoilEnviroCARS is supported by the National Science Foundation – Earth Sciences (EAR-0217473), Department of Energy - Geosciences (DE-FG02-94ER14466) and the State of Illinois. Use of the APS was supported by the U. S. Department of Energy, Basic Energy Sciences, Office of Science, under Contract No. W-31-109-Eng-38. This research was partially supported by COMPRES, the Consortium for Materials Properties Research in Earth Sciences under NSF Cooperative Agreement EAR 01-35554. This work was supported by NSF grants EAR 0309486 (DLH) and EAR 0600140 (AJC).

References

Alfè, D., Gillan M. J. and Price G. D., 2002. Composition and temperature of Earth's core constrained by combining ab initio calculations and seismic data. Earth Planet. Sci. Lett., 195: 91-98.

Anders, E. and Grevesse, N., 1989. Abundances of the elements: Meteoritic and solar. Geochim. Cosmochim. Acta, 53: 197-214.

Anderson, O. L. and Duba, A., 1997. Experimental melting curve of iron revisited. J. Geophys. Res., 102: 22659-22670.

Andrault, D., Morard, G., Bolfan-Casanova, N., Ohtaka, O., Fukui, H., Arima, H., Guignot, N., Funakoshi, K., Lazor, P. and Mezouar, M., 2007. Study of partial melting at high pressure using in situ X-ray diffraction. High Pres. Res., 26: 267-276.

Bodea, S., and Jeanloz, R., 1989. Model calculations of the temperature distribution in the laser-heated diamond anvil cell. J. Appl. Phys., 65: 4688-4692.

Boehler, R., 1993. Temperatures in the Earth's core from melting-point measurements of iron at high static pressures. Nature, 363: 534-536.

Boehler, R., 1996. Fe-FeS eutectic temperatures to 620 kbar. Phys. Earth Planet. Inter., 96: 181-186.

Brett, R. and Bell, P. M., 1969. Melting relations in the Fe-rich portion of the system Fe-FeS at 30 kb pressure. Earth Planet. Sci. Lett., 6: 479-482.

Brown, J. M., Fritz, J. N., and Hixson, R. S., 2000. Hugoniot data for iron. J. Appl. Phys., 88: 5496-5498.

Campbell, A. J., Heinz, D. L., and Davis, A. M., 1992. Material transport in laser-heated diamond anvil cell melting experiments. Geophys. Res. Lett., 19: 1061-1064.

Dreibus, G. and Palme, H., 1996. Cosmochemical constraints on the sulfur content in the Earth’s core. Geochim. Cosmochim. Acta, 60: 1125-1130.

Fei, Y., Bertka, C. M., and Finger, L. W., 1997. High pressure iron sulfur compound, Fe_3S_2, and melting relations in the Fe-FeS system. Science, 275: 1621-1623.

Fei, Y., Li, J., Bertka, C. M., and Prewitt, C. T., 2000. Structure type and bulk modulus of Fe_3S, a new iron-sulfur compound, Am. Mineral., 85: 1830-1833.

Hammersley, A. P., Svensson, S. O., Hanfland, M., Fitch, A. N., and Hausermann, D., 1996. Two-dimensional detector software: From real detector to idealised image or two-theta scan. High Pres. Res., 14: 235-248.

Heinz, D. L. and Jeanloz, R., 1987a. Temperature measurements in the laser-heated diamond cell. In: M. H. Manghnani and Y. Syono (Editors). High-Pressure Research in Mineral Physics. Terra Scientific Publishing, Tokyo / American Geophysical Union, Washington. pp. 113-127.

Heinz, D. L. and Jeanloz, R., 1987b. Measurement of the melting curve of $Mg_{0.9}Fe_{0.1}SiO_3$ at lower mantle conditions and its geophysical implications. J. Geophys. Res., 92: 11437-11444.

Jeanloz, R. and Richter, F. M., 1979. Convection, composition and the thermal state of the lower mantle. J. Geophys. Res., 84: 5497-5504.

Kiefer, B., and Duffy, T. S., 2005. Finite element simulations of the laser-heated diamond-anvil cell. J. Appl. Phys., 97: 114902.

Li, J. and Fei, Y., 2003. Experimental constraints on core composition. In: R. W. Carlson (Editor). Treatise on Geochemistry, Vol. 2. Elsevier, New York. pp. 521-546.

Li, J., Fei, Y., Mao, H. K., Hirose, K. and Shieh, S. R., 2001. Sulfur in the Earth's inner core. Earth Planet. Sci. Lett., 193: 509-514.

Mao, H. K., Bell, P. M., Shaner, J. W., and Steinberg, D. J., 1978. Specific volume measurements of Cu, Mo, Pd, and Ag and calibration of the ruby R1 pressure gauge from 0.06 to 1 Mbar. J. Appl. Phys., 49: 3276-3283.

Mao, H. K., Wu, Y., Chen, L. C., Shu, J. F., and Jephcoat, A. P., 1990. Static compression of iron to 300 GPa and $Fe_{0.8}Ni_{0.2}$ alloy to 260 GPa - Implications for composition of the core. J. Geophys. Res., 95: 21737-21742.

Massalski, T. B., Okamoto, H., Subramanian, P. R. and Kacprzak, L., 1990. Binary Alloy Phase Diagrams, 2nd Ed., ASM International, Materials Park, Ohio.

Masters, G., and Gubbins, D., 2003. On the resolution of density within the Earth. Phys. Earth Planet. Inter., 140: 159-167.

McDonough, W.F., 2003. Compositional Model for the Earth's Core. In: R. W. Carlson (Editor). Treatise on Geochemistry, vol. 2, Elsevier Ltd. pp. 547-568.

Morishima, H., and Yusa, H., 1998. Numerical calculations of the temperature distribution and the cooling speed in the laser-heated diamond anvil cell. J. Appl. Phys., 83: 4572-4577.

Panero, W., and Jeanloz, R., 2001. The effect of sample thickness and insulation layers on the temperature distribution in the laser-heated diamond cell. Rev. Sci. Instrum., 72: 1306-1308.

Panero, W., and Jeanloz, R., 2002. X-ray diffraction patterns from samples in the laser-heated diamond anvil cell. J. Appl. Phys., 91: 2769-2778.

Ryzhenko, B. and Kennedy, G. C., 1973. The effect of pressure on the eutectic in the system Fe-FeS. Am. J. Sci., 273: 803-810.

Seagle, C. T., Campbell, A. J., Heinz, D. L., Shen, G., and Prakapenka, V. B., 2006. Thermal equation of state of Fe_3S and implications for sulfur in Earth's core. J. Geophys. Res., 111: B06209.

Shen, G., Lazor, P., and Saxena, S. K,.1993. Melting of wüstite and iron up to pressures of 600 kbar. Phys. Chem. Minerals, 20: 91-96.

Shen, G., Mao, H. K., Hemley, R. J., Duffy, T. S., and Rivers, M. L., 1998. Melting and crystal structure of iron at high pressures and temperatures. Geophys. Res. Lett., 25: 373-376.

Shen, G., Rivers, M. L., Wang, Y., and Sutton, S. R., 2001. Laser heated diamond cell system at the Advanced Photon Source for in situ X-ray measurements at high pressure and temperature. Rev. Sci. Instrum., 72: 1273-1282.

Shen, G., Prakapenka, V. B., Rivers, M. L., and Sutton, S. R., 2004. Structure of liquid iron at pressures up to 58 GPa, Phys. Rev. Lett., 92: 185701.

Shen, G., Prakapenka, V. B., Eng, P., Rivers, M. L., and Sutton, S. R., 2005. Facilities for high pressure research with the diamond anvil cell at GSECARS. J. Synchrotron Radiat., 12: 642-649.

Usselman, T. M., 1975. Experimental approach to the state of the core: part I. The liquidus relations of the Fe-rich portion of the Fe-Ni-S system from 30 to 100 kb. Am. J. Sci., 275: 278-290.

Williams, Q. and Jeanloz, R., 1990. Melting relations in the iron-sulfur system at ultra-high pressures: Implications for the thermal state of the Earth. J. Geophys. Res., 95: 19299-19310.

Williams, Q., Jeanloz, R., Bass, J., Svendsen, B. and Ahrens, T. J., 1987. The melting curve of iron to 250 GPa: A constraint on the temperature at Earth's center. Science, 236: 181-187.

Williams, Q., Knittle, E., and Jeanloz, R., 1991. The high-pressure melting curve of iron: A technical discussion. J. Geophys. Res., 96: 2171-2184.

Figure Captions

Figure 1. Previous results from high pressure melting studies in the Fe-FeS system. Gray curve: Usselman, 1975; dotted curve: Williams and Jeanloz, 1990; dashed curve: Boehler, 1996; solid curve: Fei et al. (1997; 2000) and Li et al. (2001).

Figure 2. Modelled temperature distribution in an opaque diamond anvil cell sample that is laser heated on both sides. In this model identical Gaussian temperature distributions are imposed on two surfaces of the sample, with a peak temperature of 2000 K (1700 K above ambient). The sample thickness (vertical) $d = 7\ \mu$m, and the beam diameter $w = 15\ \mu$m; only the central 30 μm of the solution is shown. The dotted lines indicate the width of the synchrotron X-ray beam (5 μm). For these parameters, within the volume probed by the X-ray beam the temperature increase ($T-T_{ambient}$) at the sample midplane is 6% lower than that measured at the surface. The temperature scale in the image has been adjusted for high contrast in the region of interest; lower axial gradients exist in the cooler portions of the laser heated spot.

Figure 3. X-ray diffraction spectra of a Fe+Fe_3S mixture during and after laser heating in a diamond anvil cell. NaCl was used as a pressure medium / insulator. The 2-dimensional detector image has been caked into a rectilinear projection; the horizontal axis is the scattering angle (2θ), and the vertical axis is the azimuthal angle around the 2θ=0 direction. Vertical bars are used to indicate positions of Fe_3S, hcp-Fe, and B2-NaCl diffraction peaks. The data collection sequence proceeds from top to bottom. Prominent

Fe_3S peaks in the 1710 K diffraction spectrum disappeared in the partially molten sample at 2100 K, and then they reappeared upon quench to 300 K.

Figure 4. Melting data in the Fe-S system at high pressure. Previous results using both the multi-anvil press (Fei et al., 1997; 2000; Li et al., 2001) and the laser heated diamond anvil cell (Boehler, 1996) are compared to our results. Two experimental melting curves of pure Fe (Boehler, 1993; Shen et al., 1998) are also shown for reference.

Figure 5. Compositions in melting experiments in the Fe-FeS system. Filled circles: eutectic temperatures determined from multi-anvil experiments (Fei et al., 1997; 2000; Li et al., 2001); gray line: pressure range and composition of starting material used by Boehler et al. (1996); large open squares: starting compositions used in this study; small open squares: phases observed identified by X-ray diffraction of quenched partially melted samples in this study. All of the partial melts in this study were solid Fe + sulfide melt; the presence of Fe_3S upon quench indicates a Fe-Fe_3S eutectic extending to 60 GPa.

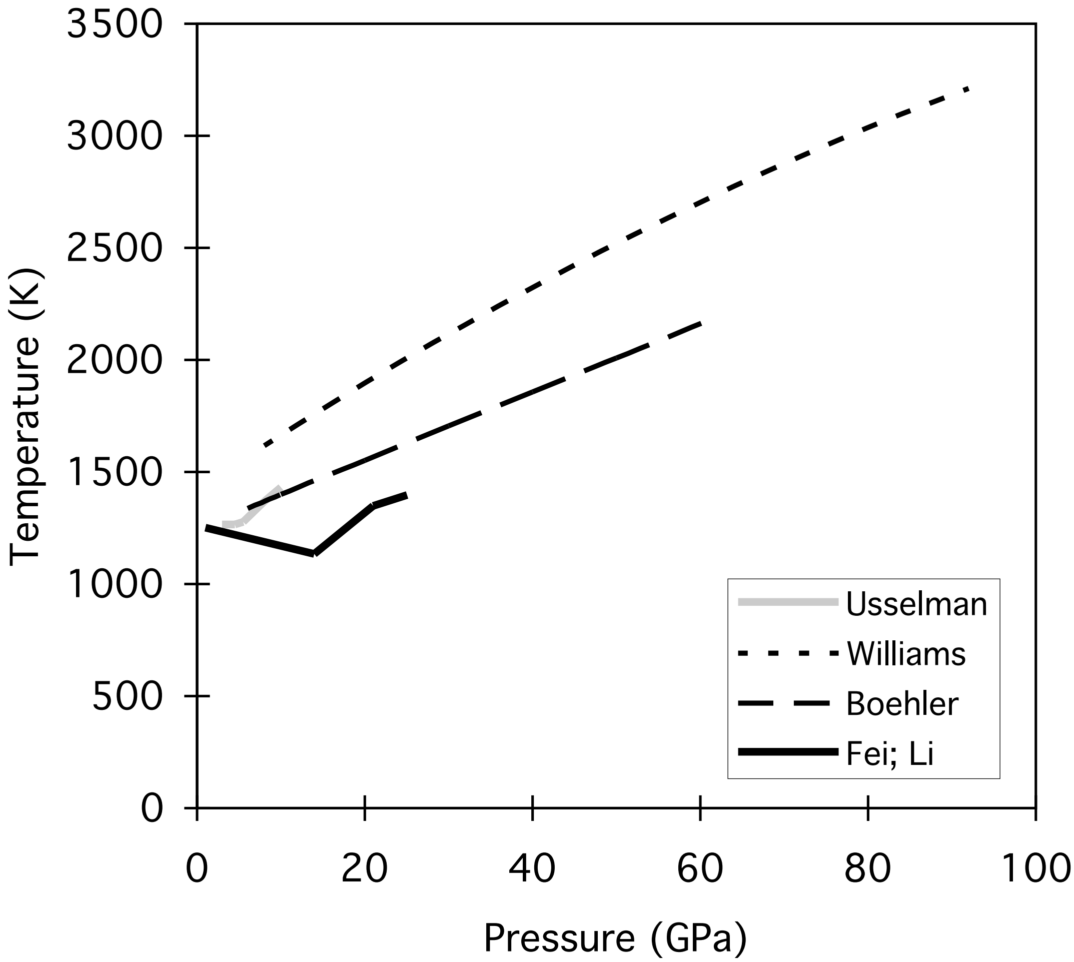
3500
3000
2500
2000
1500
1000
500
0
Temperature (K)
0
20
40
60
80
100
Pressure (GPa)
Usselman
Williams
Boehler
Fei; Li

Figure 1

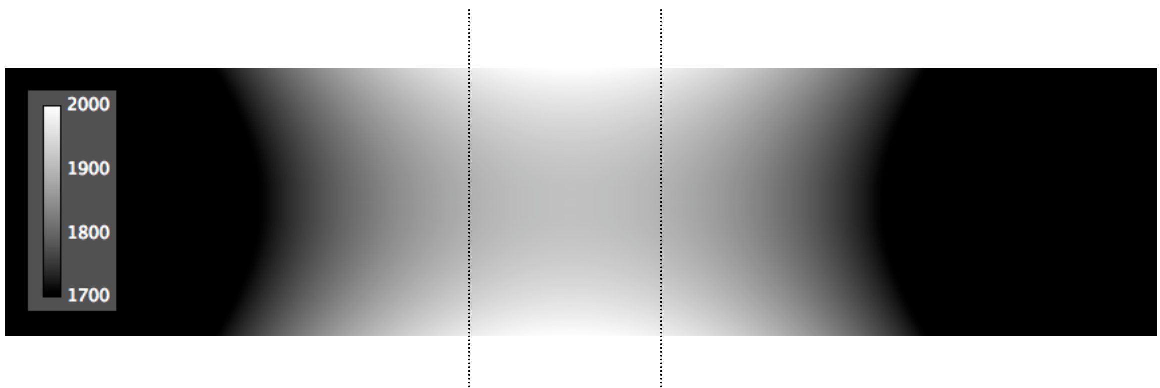

Figure 2

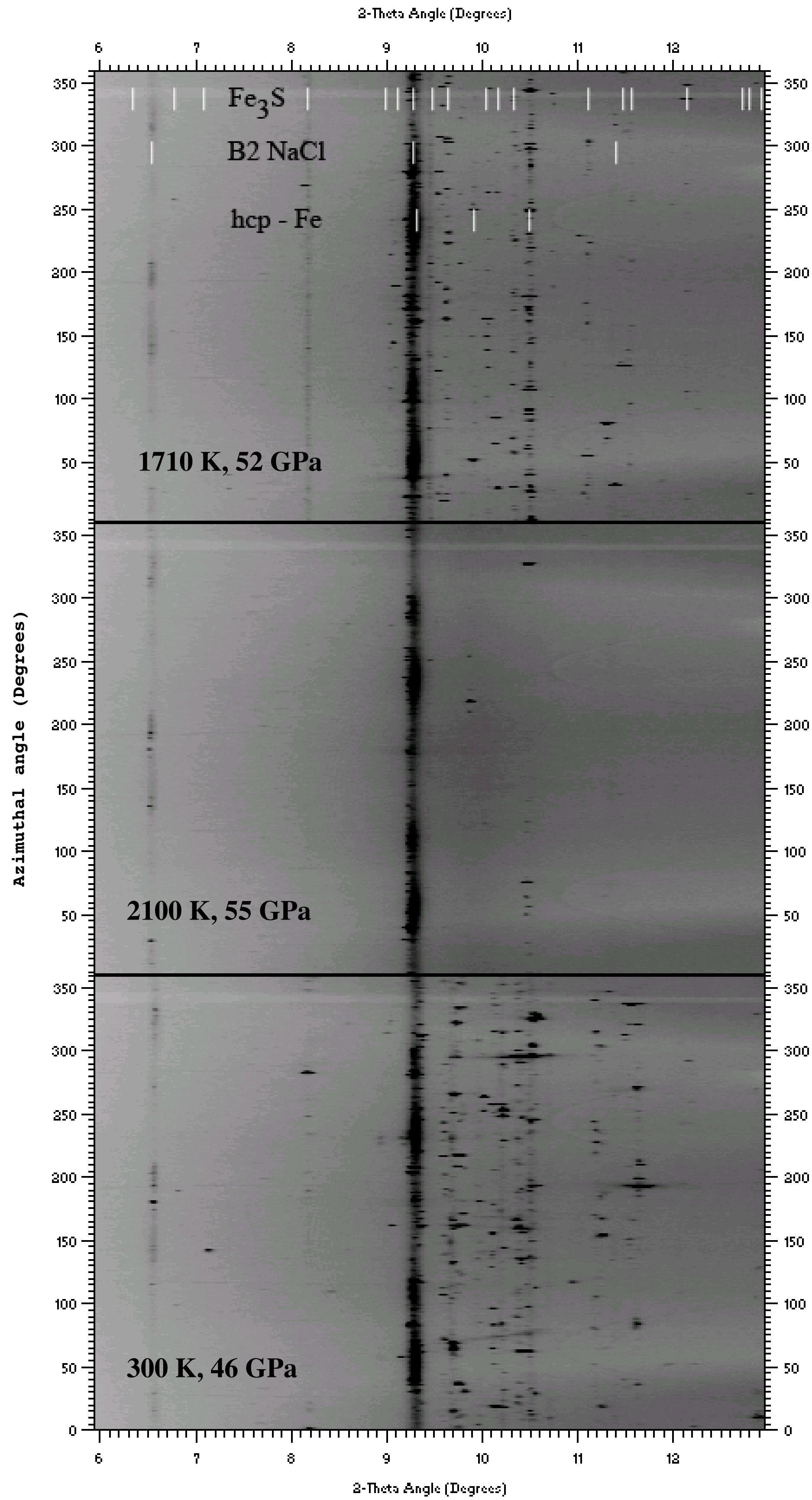
2-Theta Angle (Degrees)
Azimuthal angle (Degrees)
Fe3S
B2 NaCl
hcp - Fe
1710 K, 52 GPa
2100 K, 55 GPa
300 K, 46 GPa

Figure 3

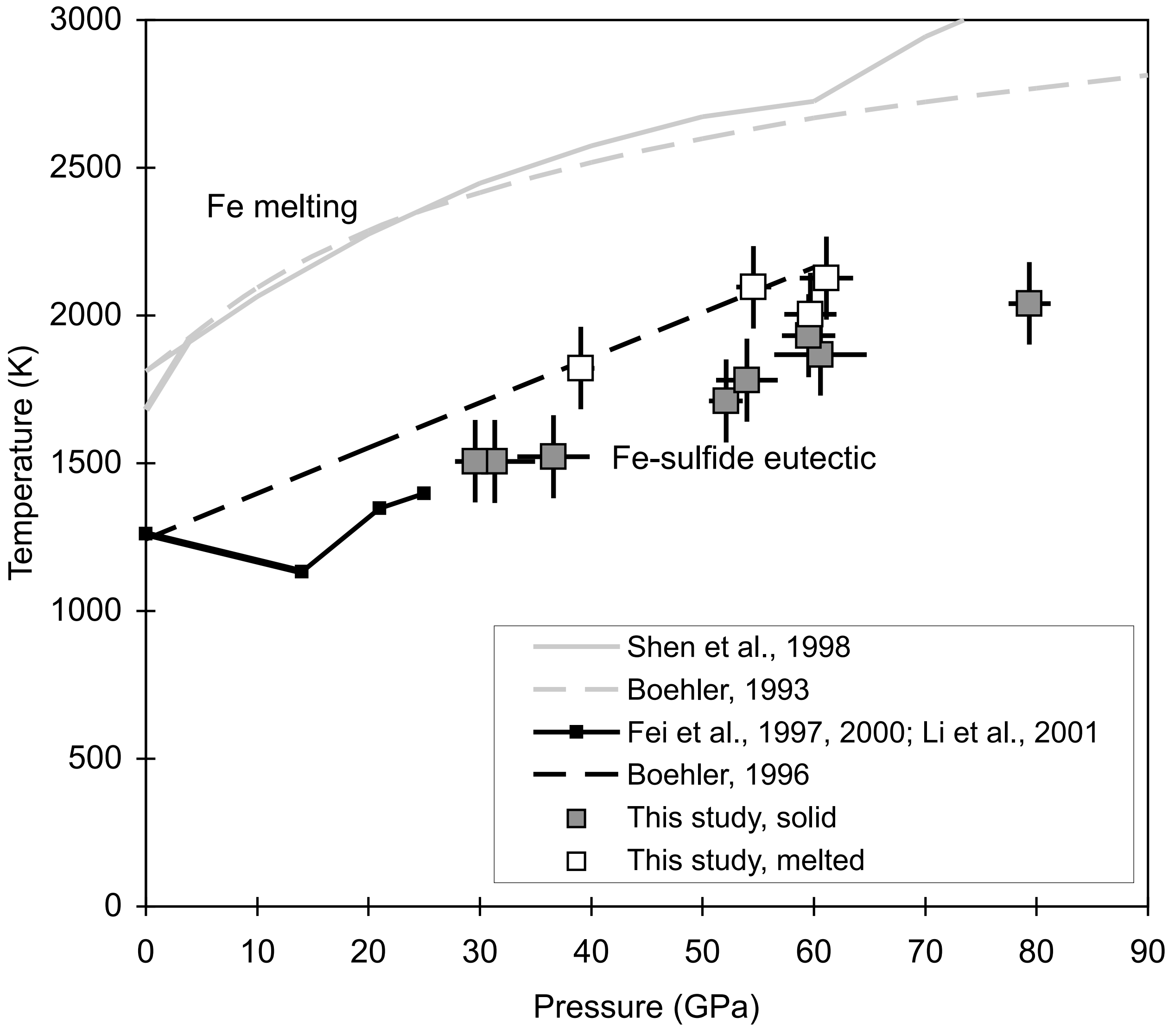
3000
2500
2000
1500
1000
500
0
Temperature (K)
0
10
20
30
40
50
60
70
80
90
Pressure (GPa)
Fe melting
Fe-sulfide eutectic
Shen et al., 1998
Boehler, 1993
Fei et al., 1997, 2000; Li et al., 2001
Boehler, 1996
This study, solid
This study, melted

Figure 4

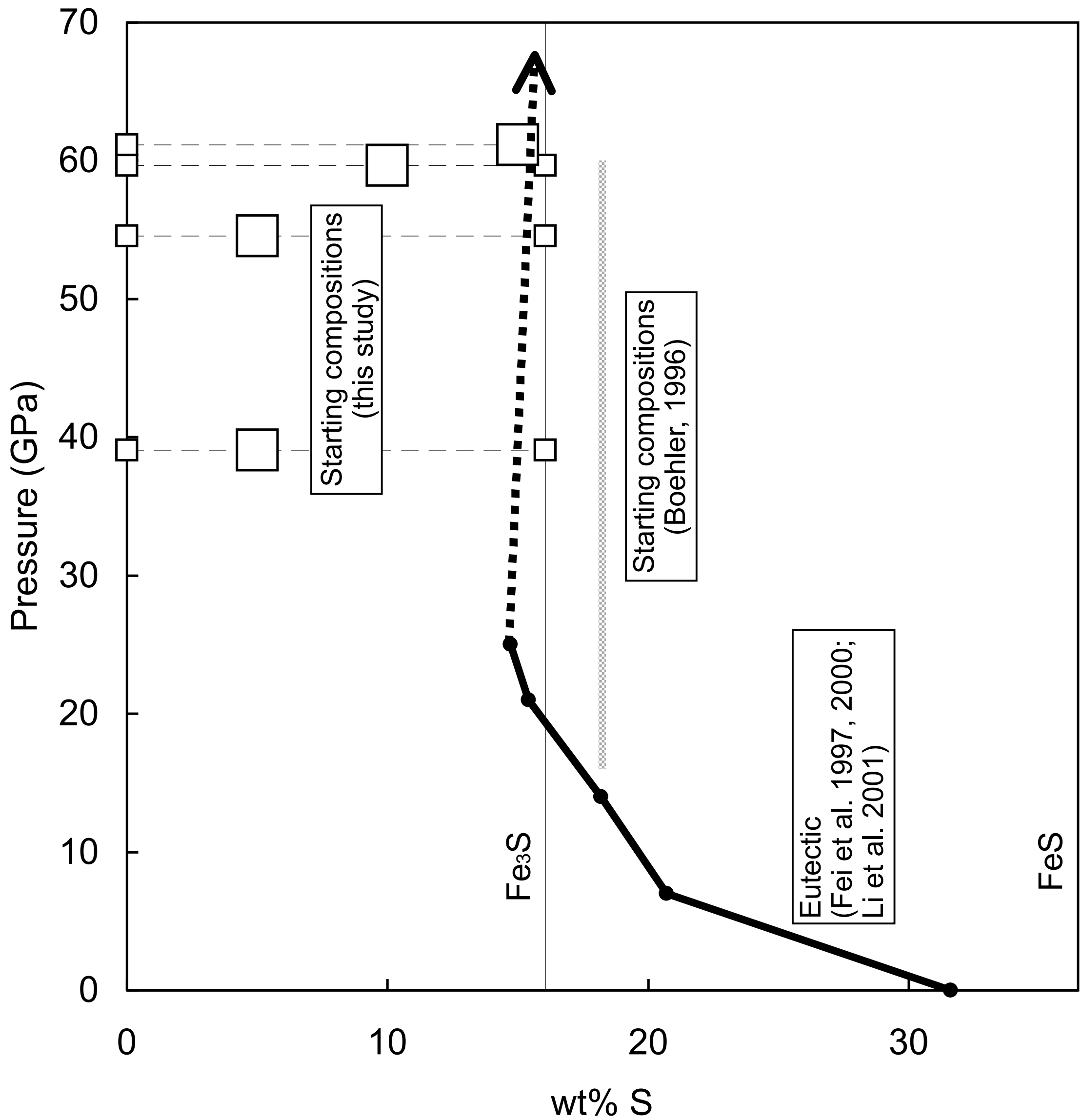

Pressure (GPa)
wt% S
0
10
20
30
40
50
60
70
0
10
20
30
Starting compositions
(this study)
Starting compositions
(Boehler, 1996)
Eutectic
(Fei et al. 1997, 2000;
Li et al. 2001)
Fe3S
FeS

Figure 5

Table 1. High pressure melting data for the Fe-Fe_3S system.

Lower Bounds on Eutectic Temperature:					
Starting wt% S	Pressure, GPa	Temperature, K	*a* of hcp-Fe, Å	*c* of hcp-Fe, Å	*V* of hcp-Fe, cm^3/mol
15	29.6 ± 1.2	1520 ± 140	2.4489 ± 0.0001	3.9672 ± 0.0003	6.204 ± 0.001
15	31.4 ± 3.6	1510 ± 140	2.4563 ± 0.0031	3.9153 ± 0.0147	6.160 ± 0.026
5	36.6 ± 3.2	1520 ± 140	2.4345 ± 0.0030	3.9101 ± 0.0119	6.043 ± 0.021
5	52.1 ± 1.5	1710 ± 140	2.3938 ± 0.0005	3.8731 ± 0.0018	5.787 ± 0.003
15	54.0 ± 2.8	1780 ± 140	2.3887 ± 0.0020	3.8778 ± 0.0095	5.770 ± 0.016
15	59.5 ± 2.4	1930 ± 140	2.4082 ± 0.0008	3.7749 ± 0.0084	5.709 ± 0.013
10	60.6 ± 4.2	1870 ± 140	2.3784 ± 0.0030	3.8507 ± 0.0160	5.680 ± 0.026
15	79.4 ± 1.9	2040 ± 140	2.3491 ± 0.0001	3.7880 ± 0.0003	5.451 ± 0.001

Upper Bounds on Eutectic Temperature:					
Starting wt% S	Pressure, GPa	Temperature, K	*a* of hcp-Fe, Å	*c* of hcp-Fe, Å	*V* of hcp-Fe, cm^3/mol
5	39.0 ± 1.2	1820 ± 140	2.4467 *	3.8880 *	6.069 *
5	54.6 ± 1.6	2100 ± 140	2.3971 ± 0.0009	3.8883 ± 0.0018	5.826 ± 0.004
10	59.7 ± 2.3	2000 ± 140	2.3822 ± 0.0014	3.8656 ± 0.0075	5.720 ± 0.012
15	61.1 ± 2.4	2130 ± 140	2.4076 ± 0.0008	3.7854 ± 0.0085	5.722 ± 0.013

* No uncertainty is given when only two diffraction lines from hcp-Fe were observed.